A Mechanistic Study of the Lewis Base-Directed Cycloaddition of 2-Pyrones and Alkynylboranes

Damien F. P. Crépin,[†] Joseph P. A. Harrity,*,[†] Julong Jiang,[†] Anthony J. H. M. Meijer,*,[†] Anne-Chloé M. A. Nassoy,[†] and Piotr Raubo[‡]

[†]Department of Chemistry, University of Sheffield, Sheffield S3 7HF, U.K.
[‡]Research and Development, AstraZeneca, Alderley Park, Macclesfield SK10 4TG, U.K.

Ⓦ Web-Enhanced Feature Ⓢ Supporting Information

ABSTRACT: Significant rate enhancements in the Diels−Alder reaction of alkynes and 2-pyrones bearing a Lewis basic group are observed when a combination of alkynyltrifluoroborates and $BF_3 \cdot OEt_2$ is used. This process generates functionalized aromatic compounds with complete regiocontrol. The observed rate enhancement was studied by density functional theory methods and appears to originate from coordination of the diene substrate to a mixture of alkynylborane intermediates, followed by a Lewis acid-mediated product equilibration step. Evidence for this mechanism is presented, as is the enhanced promotion of the cycloaddition via the use of alternative Lewis acid promoters.
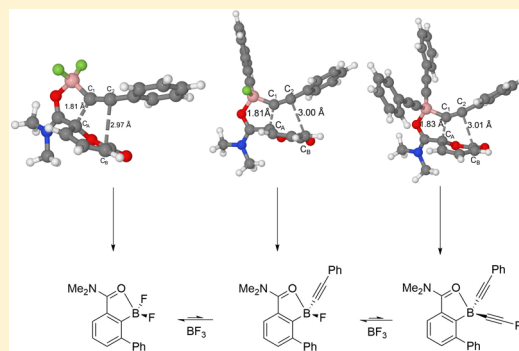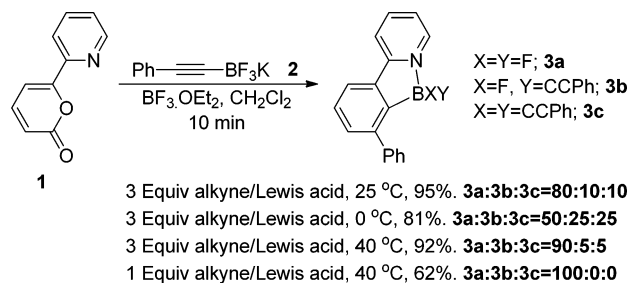
INTRODUCTION

The Diels−Alder cycloaddition of 2-pyrones represents an efficient method of generating functionalized cyclohexenes[1] and was first described by Diels and Alder over 80 years ago.[2] This reaction also offers an effective method for the synthesis of highly substituted aromatic compounds when alkynes are employed, whereby the intermediate cycloadduct undergoes rapid retro-cycloaddition and expulsion of carbon dioxide.[3] A range of alkynes are known to participate in this process, including those bearing hydrocarbon, ester, ketone,[3] boronate,[4] stannane,[5] and silyl[6] groups. A significant challenge in this chemistry is the requirement of high reaction temperatures over extended time periods and variable reaction regiocontrol. Such limitations have been addressed only by the use of very reactive dienophiles such as ynamides,[7] thereby restricting the scope of products that can be generated by this strategy.

Recent studies in our laboratories have sought to address the high temperatures required in [4 + 2] cycloaddition reactions of aromatic dienes by virtue of a Lewis acid−base complex-induced promotion of this process.[8] This approach has the added advantage of generating compounds with complete regiocontrol. We have developed a mild and regioselective synthesis of aromatic difluoroboranes via the cycloaddition of 2-pyrones with in situ-generated alkynyldifluoroboranes.[9] As outlined in Scheme 1, our optimization studies highlighted some unexpected trends. The reaction required the use of 3 equiv of both the alkyne substrate and the Lewis acid fluorophile for optimal yields. Moreover, alkynylated byproducts were observed when the reaction was conducted under ambient conditions. In this context, the mild Diels−Alder cycloaddition of 1,3-dienes with vinyl- and alkynylbor-

Scheme 1. Lewis Acid-Promoted Cycloaddition of 2-Pyrones

3 Equiv alkyne/Lewis acid, 25 °C, 95%. **3a:3b:3c=80:10:10**
3 Equiv alkyne/Lewis acid, 0 °C, 81%. **3a:3b:3c=50:25:25**
3 Equiv alkyne/Lewis acid, 40 °C, 92%. **3a:3b:3c=90:5:5**
1 Equiv alkyne/Lewis acid, 40 °C, 62%. **3a:3b:3c=100:0:0**

anes has also been established by Singleton and co-workers.[10] These processes take place at ambient temperature and with excellent levels of regiocontrol via a [4 + 3] transition structure.

The directed cycloaddition reaction raised some interesting questions with regard to the reaction mechanism: (1) Is Lewis acid activation of the 2-pyrone operating as well as or instead of the directed cycloaddition? (2) Does the directing group control the reaction regioselectivity or does the reaction proceed via the Singleton [4 + 3] mechanism? (3) How are the alkynylated byproducts formed? In order to understand this reaction more clearly, we undertook theoretical density functional theory (DFT) calculations of the cycloaddition reaction in order to establish a clearer picture of this unusually rapid cycloaddition process. Theoretical studies of Lewis acid-promoted Diels−Alder reactions have been reported in the literature,[11] though not on these systems. We report herein our

Scheme 2. Enthalpy Profile for the Ligand Exchange Reaction between Two Alkynylborane (Monomer IM) Molecules in DCM; the Inset Shows the Structure of Transition State TS1M, Where the Bonds Forming Are Dashed
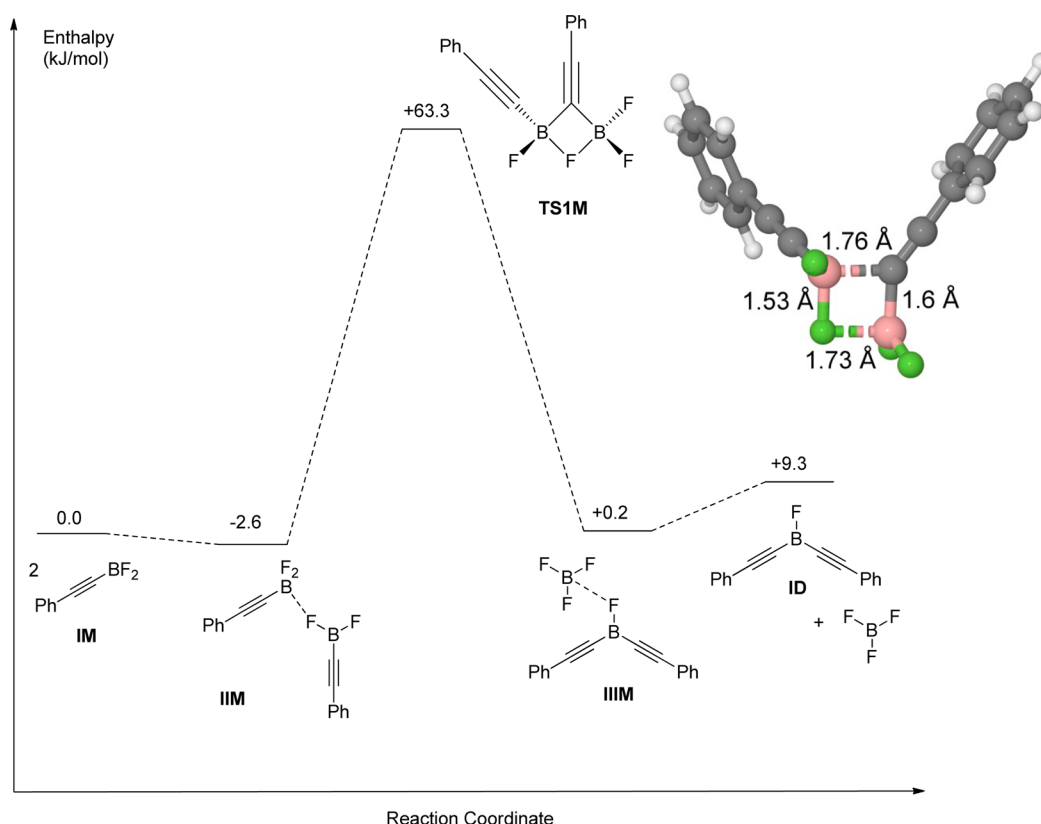
findings and their application in improving the Lewis acid-promoted cycloaddition reaction.

COMPUTATIONAL METHODS

All of the calculations were performed using DFT with the B3LYP hybrid functional[12,13] as implemented in Gaussian 09.[14] The 6-311G(d,p) basis set was used for H, C, N, O, B, F, and Cl atoms. All of the reactant, intermediate, transition state, and product structures were fully optimized without any symmetry restrictions. Transition states were located using the QST3 algorithm[15−17] or the Berny algorithm.[18]

Frequency calculations were carried out to characterize all of the optimized structures as local minima or transition states. Transition states were identified by having one imaginary frequency. An intrinsic reaction coordinate (IRC)[19] calculation was performed for each transition state to ensure that it connected the correct reactants and products. Solvent effects were included in all of the calculations through the IEF-PCM[20−22] model as implemented in Gaussian 09[14] with dichloromethane (DCM) as the solvent. The atomic charges were fitted to the electrostatic potential energy (ESP) following the Merz–Kollman scheme.[23,24] All of the enthalpies and free energies quoted below were evaluated at 298.15 K.

THEORETICAL RESULTS

Our first objective was to attempt to explore possible mechanisms for the formation of the alkynylated aromatic boranes such as **3b** and **3c** shown in Scheme 1. Our initial hypothesis involved alkyne disproportionation prior to cyclo-addition. However, Frohn and co-workers had shown that alkynyldifluoroboranes can be isolated and characterized as single compounds upon the treatment of alkynyltrifluoroborates with boron trifluoride.[25] Nevertheless, alkyne exchange between organoboranes and -borates has been reported by Negishi et al.[26] First, the ligand exchange reaction between two

(phenylethynyl)borane (**IM**) monomers was considered. Following ref 27a, the enthalpy profile for the ligand exchange reaction between two **IM** monomers is shown in Scheme 2. In nonpolar solvents like DCM, the alkynylborane forms a loosely coordinated dimer **IIM**, which results in a small enthalpy change of -2.6 kJ mol^{-1}. This prereaction complex then undergoes ligand exchange to generate bis(phenylethynyl)-borane (**ID**) and a molecule of BF$_3$. Inspection of the transition state for this process (**TS1M**) shows that this reaction involves a concerted mechanism via a four-membered ring involving two three-center two-electron bonds (Scheme 2). The enthalpy barrier for the ligand (phenylacetylide moiety) exchange between two alkynylborane molecules is calculated to be $+65.9$ kJ mol^{-1} starting from the loosely coordinated dimer **IIM**. The product of this process, **IIIM**, is again a loosely bound complex. However, it is a complex of diphenylacetylide **ID** and BF$_3$, wherein BF$_3$ prefers to bind with the fluoride of **ID**. The calculations clearly show that the formation of the bis(alkynyl)-borane from two alkynylborane molecules is an endoergic process, since the Gibbs energy increases overall by 13.2 kJ mol^{-1} relative to two individual alkynylborane molecules. Therefore, for this process to be viable it must be coupled with the Diels–Alder cycloaddition step (vide infra).

Following a similar pathway, tris(phenylethynyl)borane (**IT**) can be formed either by alkynylborane **IM**/bis(alkynyl)borane **ID** disproportionation or by ligand exchange from two bis(alkynyl)borane **ID** molecules. The likely relative concentrations of **IM** and **ID** suggest that ligand exchange via the reaction of **IM** and **ID** is more likely to happen. Thus, the intermediates and transition states along this reaction pathway were optimized. The enthalpy profile for the generation of

Scheme 3. Enthalpy Profile for the Ligand Exchange Reaction between an Alkynylborane Molecule (IM) and a Bis(alkynyl)borane Molecule (ID) in DCM
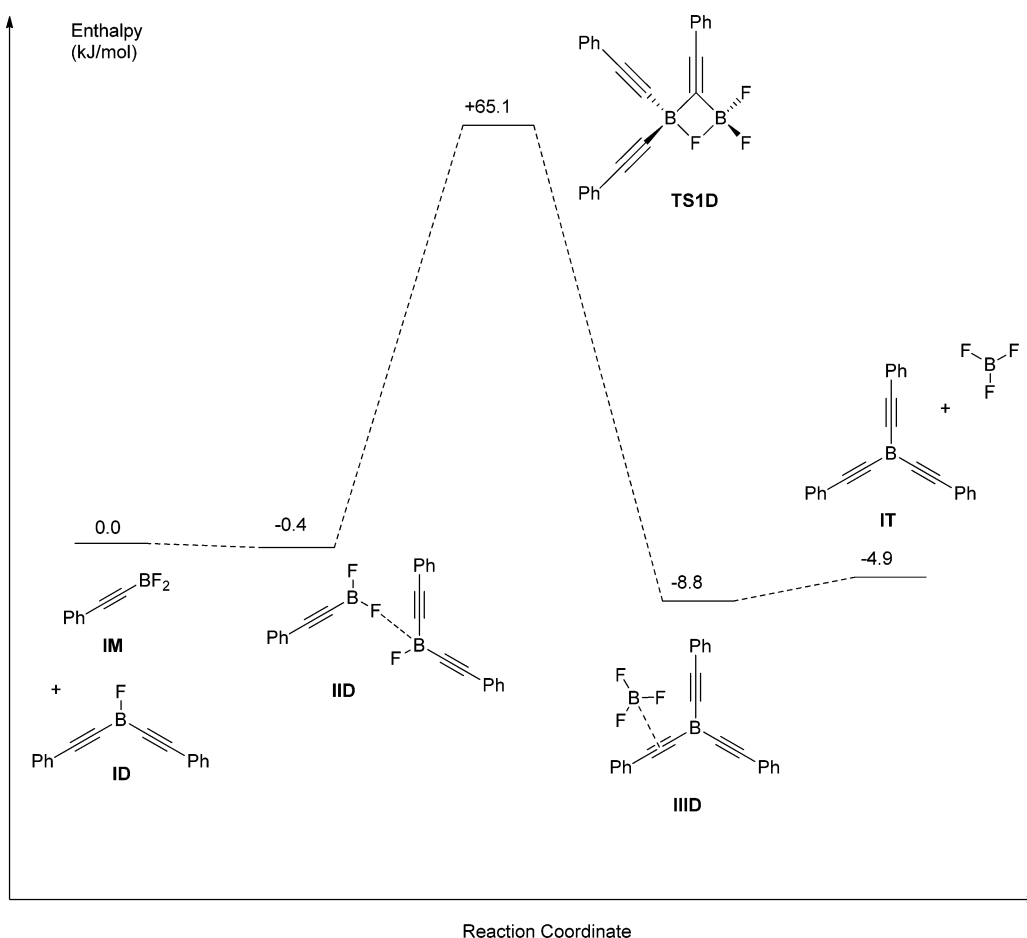
tris(alkynyl)borane **IT** is shown in Scheme 3. The enthalpy barrier for this disproportionation reaction is +65.5 kJ mol^{-1}. It again delivers a loosely coordinated product. Dissociation of this complex provides free tris(alkynyl)borane **IT**, which is available to participate in the subsequent Diels−Alder reaction. We note that in this case the overall reaction Gibbs energy is negative (−2.5 kJ mol^{-1}). Thus, our calculations show that equilibration of a series of alkynylboranes can take place and that this equilibrium favors the formation of tris(alkynyl)borane **IT** and its corresponding BF$_3$ complex **IIID**. This needs to be taken into account when the subsequent Diels−Alder reaction is studied.

Having established the potential for rapid alkyne equilibration via disproportionation, we envisaged that the cycloadduct product distribution would depend on the relative energies of the pyrone-complexed trivalent boranes as well as the activation energy of the ensuing cycloaddition. Therefore, we turned our attention to the Diels−Alder step, adopting either the alkynylborane, bis(alkynyl)borane, or tris(alkynyl)borane as the dienophile and the 2-pyrone N,N-dimethyl-2-oxo-2H-pyran-6-carboxamide (**S1**) as the diene.

The mapped enthalpy profile for the Diels−Alder reaction between alkynylborane **IM** and **S1** is shown in Scheme 4. The first step in this regiodirecting Diels−Alder reaction is the coordination of the amide carbonyl directing group of the 2-pyrone to the boron atom of the alkynylborane. This step lowers the enthalpy by 37.9 kJ mol^{-1}. The subsequent Diels−Alder reaction therefore proceeds via this prereaction complex

IM_DA_I1. Inspection of the cycloaddition transition state (**IM_DA_TS1**) shows that the Diels−Alder reaction can be described as asynchronous. Thus, the two bonds C$_1$−C$_A$ and C$_2$−C$_B$ do not form simultaneously. In the optimized structure of the transition state, the C$_1$−C$_A$ bond length is 1.81 Å while the distance between C$_2$ and C$_B$ is still as large as 2.97 Å, as is clear from Figure 1a. (An animation of this transition state is provided in the HTML version of this paper.) Thus, our calculations clearly indicate that the reaction proceeds via a directed [4 + 2] mechanism rather than the Singleton [4 + 3] mechanism.

ESP charges based on the Merz−Kollman scheme (vide infra; Table 2) clearly indicate that the C$_1$−C$_A$ bond is formed via nucleophilic attack by the C$_1$ atom of the phenylacetylide group on the C$_A$ atom of the 2-pyrone ring, leading to a polar intermediate. Such stepwise [4 + 2] cycloadditions of 2-pyrones are known and have been studied by DFT methods in the past.[27] Finally, the product of this cyclization reaction is the bridged compound **IM_DA_I2**, whose structure is shown in the inset of Scheme 4. It is worth noting that the O−C bond length of the carbonyl group in this bridged compound extends to 1.28 Å and that the N−C bond on the other hand shortens to 1.31 Å, which is quite similar to the length of a C=N double bond. However, this bridged compound **IM_DA_I2** is not stable toward release of CO$_2$. The enthalpy barrier for the CO$_2$ release and rearrangement of the aromatic ring is +39.2 kJ mol^{-1}, while the enthalpy change for this step is −238.3 kJ mol^{-1}.

Scheme 4. Enthalpy Profile for the Regiodirecting Diels−Alder Reaction between Alkynylborane IM and 2-Pyrone S1 in DCM; the Inset Shows the Structure of IM_DA_I2
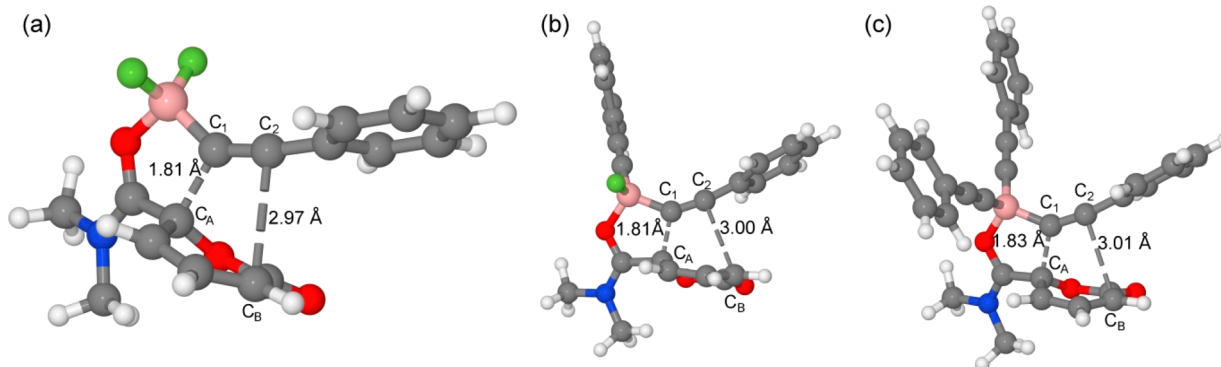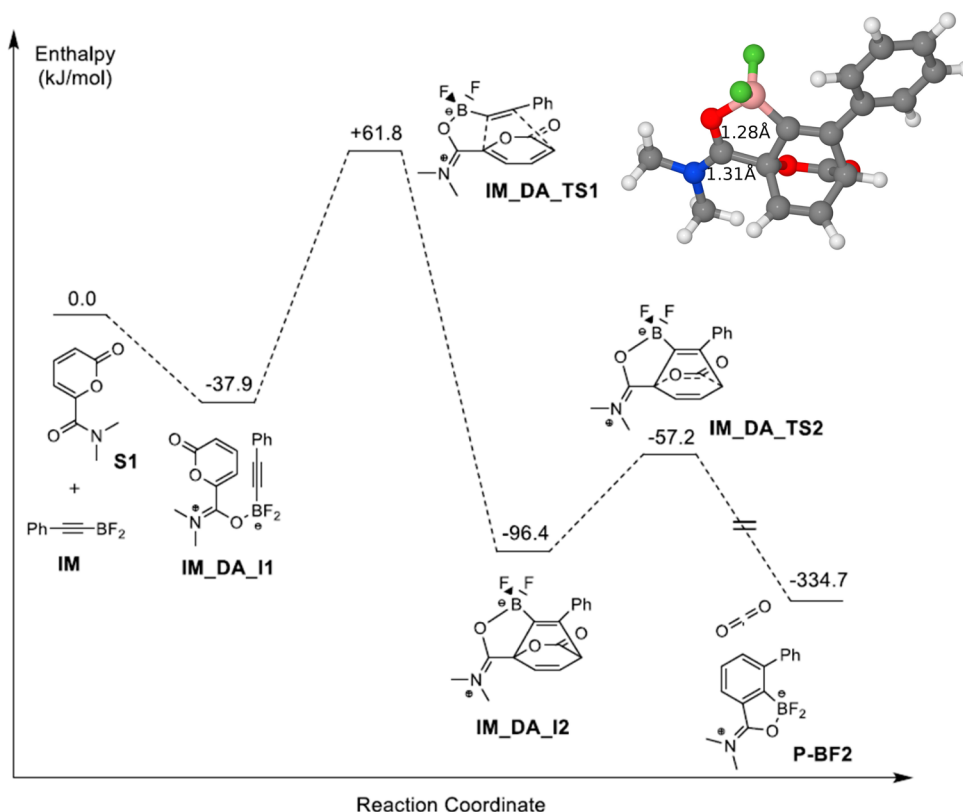

Figure 1. Transition states of the three Diels−Alder reactions: (a) reaction of **IM** with **S1**; (b) reaction of **ID** with **S1**; (c) reaction of **IT** with **S1**.

We also studied the related pathways of this regioselective Diels−Alder reaction starting with bis(alkynyl)borane **ID** and tris(alkynyl)borane **IT**. The corresponding enthalpy profiles are shown in Schemes 5 and 6. Comparison of Schemes 5 and 6 to each other and to Scheme 4 shows some similarities and some differences among the three reactions. For Scheme 5, as for Scheme 4, the initial step is the formation of a prereaction complex, and it should be noted that the enthalpy change for this step in Scheme 4 is about twice as large as that for this step in Scheme 5. It is therefore not surprising that the formation of this prereaction complex is actually endothermic for **IT**, as is evident from Scheme 6. On the other hand, the transition states of the three schemes (Figure 1) show that all three Diels−Alder reactions can be described as asynchronous, forming one C−C bond before the second one. In all three cases, the bridged product of the DA reaction is not stable and should lose CO_2

quite easily, given the relative enthalpy barrier of ∼40 kJ mol^{-1} with a large reaction exothermicity in each case.

To compare these reactions quantitatively, it is necessary to define an effective barrier in each case. This can be less than straightforward, particularly when there are multiple transition states and minima to consider. Thus, in order to assign the barriers consistently, we used the energetic span (ES) model developed by Kozuch and co-workers.[28−30] Within the ES model, the crucial states (i.e., stationary points on the potential energy surface) of the system are those that give the maximum energy difference between a minimum and a subsequent transition state, that is, the ones that give the maximum effective barrier or energetic span for the reaction.[28−30] In Scheme 4, those states are **IM_DA_I1** and **IM_DA_TS1**, which are termed the turnover-determining intermediate (TDI) and turnover-determining transition state (TDTS), respec-

Scheme 5. Enthalpy Profile for the Regiodirecting Diels–Alder Reaction between Bis(alkynyl)borane ID and 2-Pyrone S1
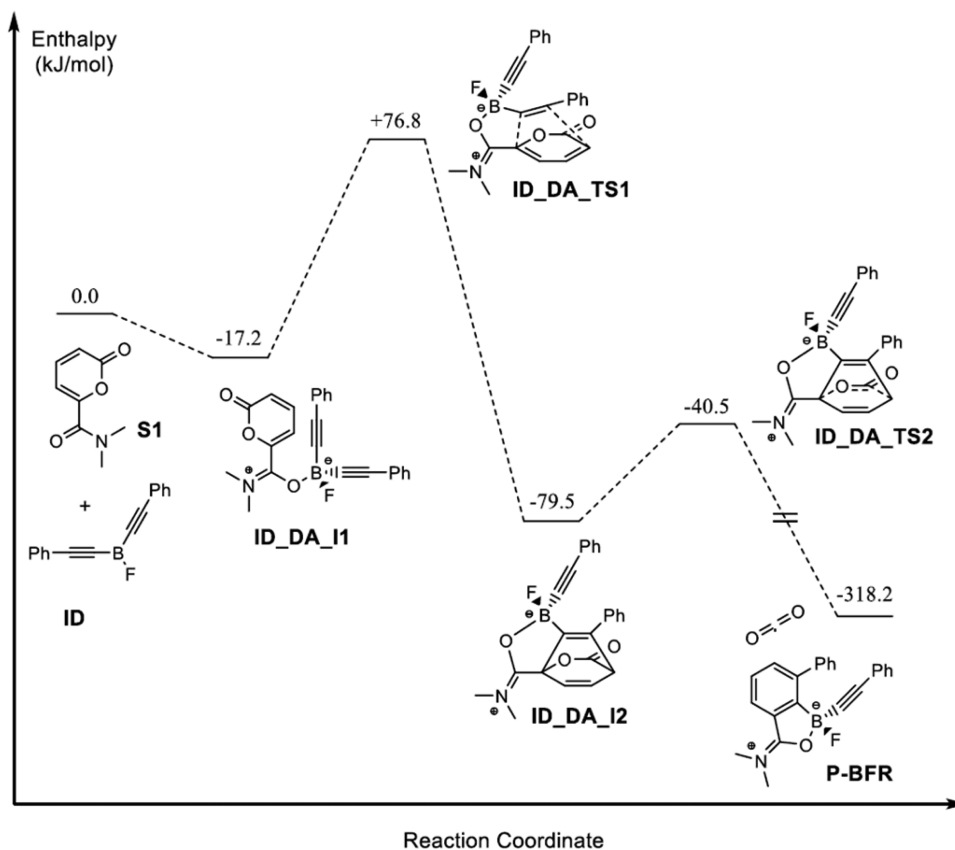
Scheme 6. Enthalpy Profile for the Regiodirecting Diels–Alder Reaction between Tris(alkynyl)borane IT and 2-Pyrone S1
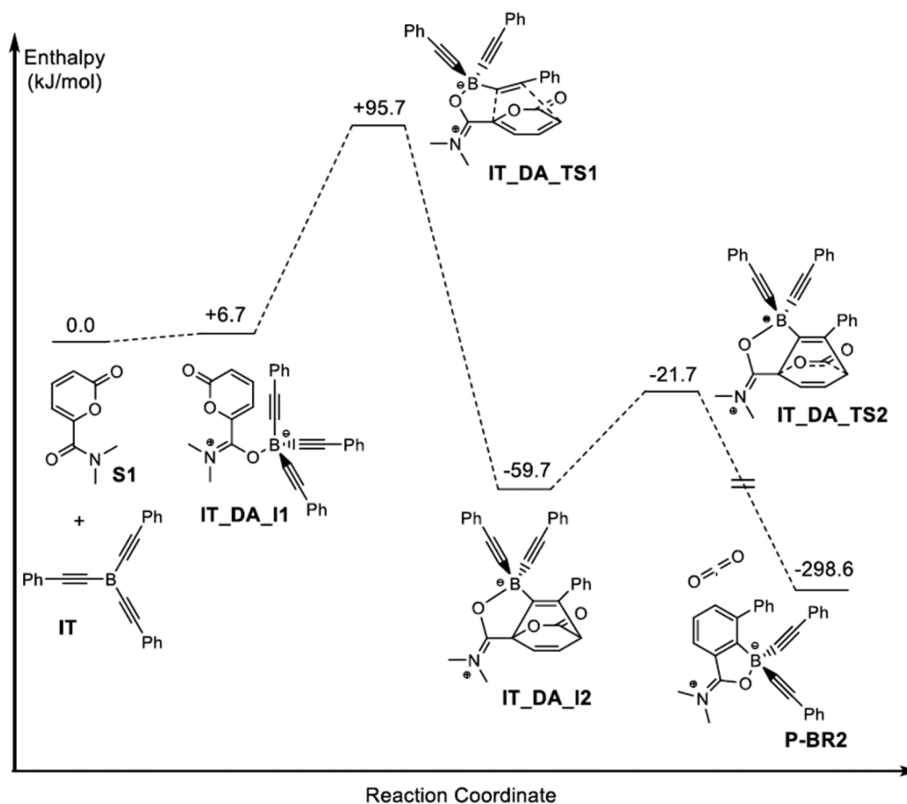
tively. As a result, the effective enthalpy barrier for this reaction is +99.7 kJ mol^{-1}.

In Schemes 5 and 6, it is clear that the transition state of the cyclization step (i.e., **ID_DA_TS1** and **IT_DA_TS1**, respectively) is the TDTS. In Scheme 5, the prereaction complex **ID_DA_I1** is the TDI, whereas in Scheme 6, the separated reactants form the TDI. Therefore, the effective barriers (i.e., the enthalpy differences between the TDTS and TDI) in Schemes 5 and 6 are calculated to be +94.0 and +95.7 kJ mol^{-1}, respectively.

From the combined results of our theoretical studies of both the ligand exchange pathway and the Diels–Alder reaction, it is now clear why a mixture of aromatic boranes is formed. Compared with the cycloaddition step, the ligand exchange process allows for rapid equilibration of the various alkynylborane intermediates. The relative rates of cycloaddition of these alkynylboranes then determine the distribution of initial cycloadducts. As shown by the data in Table 1, the

Table 1. Effective Barriers (Energetic Spans) for the Diels–Alder Reactions with Different Dienophiles

Dienophile	$\Delta G^{\ddagger}$ (kJ mol^{-1})	Relative rate	$\Delta H^{\ddagger}$ (kJ mol^{-1})	Relative rate
alkynylborane (**IM**)	109.5	1.0	99.7	1.0
bis(alkynyl)borane (**ID**)	100.7	34.8	94.0	10.0
tris(alkynyl)borane (**IT**)	100.4	39.3	95.7	5.0

effective barrier decreases with ligand exchange of fluoride for acetylide, which means that the rate increases accordingly. If it is assumed that the reaction proceeds under kinetic control, relative reaction rates can be calculated using the Eyring equation. These results are shown in the third column of Table 1. If we assume that the changes in entropy are similar for the three reactions, then we can define a relative rate on the basis of the enthalpy alone. These relative rates are given in the fifth column of Table 1. It is clear from Table 1 that the two rate calculations give qualitatively the same results, namely that the reaction rates for **ID** and **IT** are similar to each other and much larger than the rate for **IM**.

Inspection of the enthalpy profiles in Schemes 4–6 shows a clear dependence of the enthalpy of activation on the nature of the ligands around boron. In order to rationalize this result, a Merz–Kollman ESP charge analysis was conducted, and the results for each of the four reactants are given in Table 2.

**Table 2. Merz–Kollman ESP Charges for Each of the Reactants Involved in Schemes 4–6**

Dienophile	Charge on B	Charge on C_1	Charge on C_2
alkynylborane (**IM**)	0.87	−0.37	−0.15
bis(alkynyl)borane (**ID**)	0.80	−0.43	0.0
tris(alkynyl)borane (**IT**)	0.70	−0.42	0.0
Diene	Charge on O	Charge on C_A	Charge on C_B
2-pyrone (**S1**)	−0.55	0.43	−0.64

Comparison of the charges for the three dienophiles shows that boron in each case carries a positive charge. However, with additional phenylacetylide groups, this charge is lower. Simultaneously, the negative charge on C_1 increases. Thus, if we only consider electrostatic effects, this would mean that the initial complex should become less stable with an increasing degree of substitution with phenylacetylide groups, which

indeed is confirmed by the full enthalpy profile. At the same, the increasing charge on C_1 (and decreasing charge on C_2) with increasing degree of substitution should lead to more effective nucleophilic attack by C_1 on C_A, which is apparent in the lowering of the barrier, as is clear from a comparison of Schemes 4−6. In fact, notwithstanding the fact that one cannot assume these charges to be accurate to 0.01, the slightly lower charge on C_1 for **IT** compared with **ID** suggests a slightly higher barrier, as is clear from Table 1.

The calculations shown in Table 1 suggest that the cycloadditions should provide a mixture of products favoring mono- and dialkynylated boranes. However, experimental studies show that aryldifluoroboranes are the major products. We therefore speculated that the final stage of the cycloaddition process requires a further equilibration of arylboranes and thus undertook a study of potential ligand exchange processes in the products. Interestingly, as shown in Scheme 7, the calculations

Scheme 7. Ligand (Phenylacetylide Group) Exchange Reactions of P-BR2 and P-BFR with BF$_3$
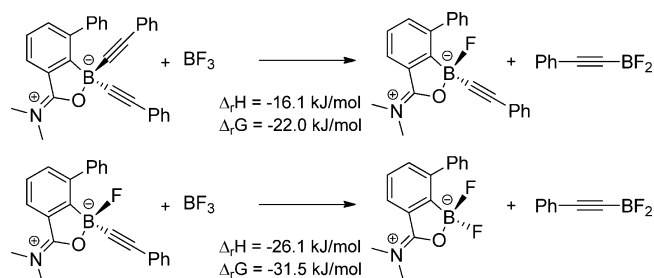

indicate that the boron trifluoride-promoted conversion of **P-BR2** via **P-BFR** to **P-BF2** is exothermic. For the first transformation from **P-BR2** to **P-BFR** Δ_rH and Δ_rG are −16.1 and −22.0 kJ mol^{-1}, respectively. For the final transformation into **P-BF2**, Δ_rH and Δ_rG are −26.1 and −31.5 kJ mol^{-1}, respectively.

While there does not appear to be a very significant driving force for the equilibration of all possible cycloadducts to the aryldifluoroborane, the presence of excess Lewis acid (remaining after consumption of the alkyne during cyclo-addition) probably serves to drive this transformation forward. To investigate this further, the enthalpy profiles for the equilibrations of mono- and dialkynylated cycloadducts were studied and are depicted in Schemes 8 and 9, respectively. Our calculations clearly show that the formation of **P-BF2** should indeed be quite facile given the low barriers, which are significantly lower than the corresponding barriers to the formation of **ID** and **IT**. Thus, our calculations clearly explain and confirm the experimental observations.

The above discussion does not consider the role of the directing group and its effect on the formation of the final products. Unfortunately, the directing group of the 2-pyrone is in such a position that the study of a nondirected reaction leading to the same products is not feasible. However, one of us previously reported a nondirected Diels−Alder reaction as a route to synthesize functionalized aromatic boronic esters, as shown in Scheme 10.[31] In the case of this nondirected cycloaddition, the reaction conditions are quite harsh and require heating at 180 °C for 18 h to drive the reaction to completion. Thus, to understand the role of the directing group and to explain the difference between the nondirected Diels−Alder reaction and the novel mild directed Diels−Alder

F

dx.doi.org/10.1021/ja501805r | J. Am. Chem. Soc. XXXX, XXX, XXX–XXX

Scheme 8. Enthalpy Profile for the Ligand Exchange Reaction between P-BR2 and BF$_3$; the Dissociation of the Final Complex Is Endothermic by 10.7 kJ mol^{-1}
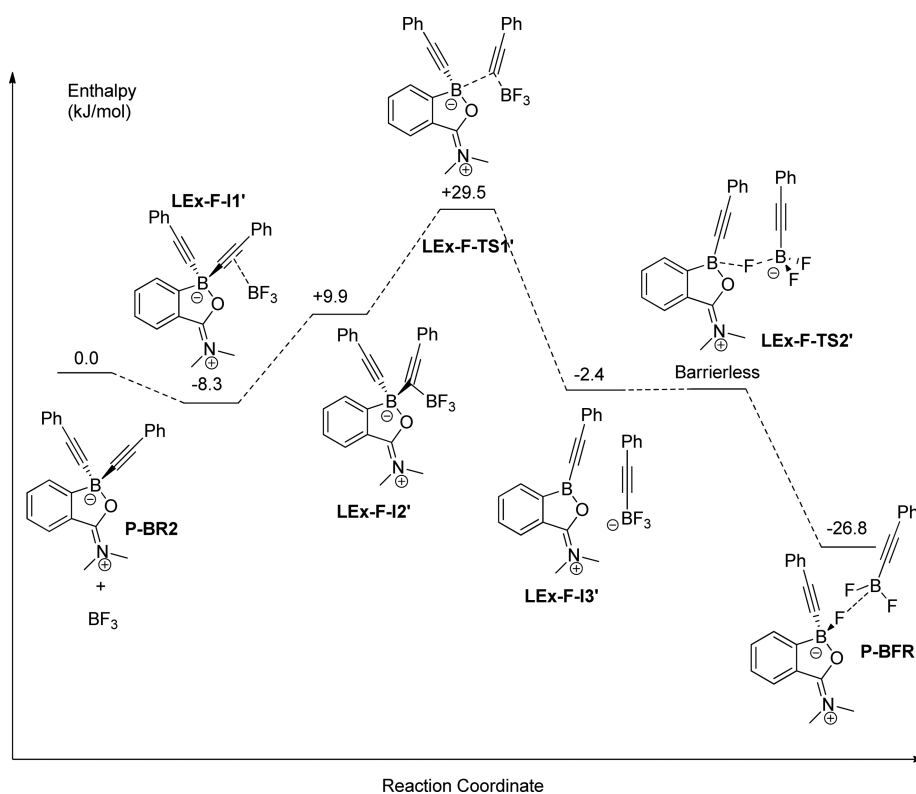
Scheme 9. Enthalpy Profile for the Ligand Exchange Reaction Between P-BFR and BF$_3$; the Dissociation of the Final Complex Is Endothermic by 7.9 kJ mol^{-1}
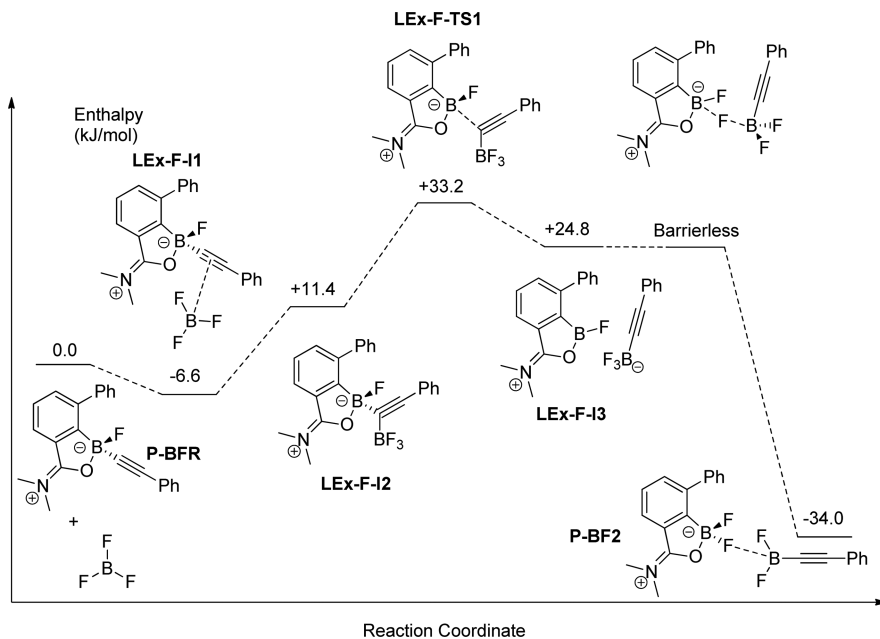

reaction, we decided to re-examine the minimum-energy path for this previously reported nondirected Diels−Alder reaction instead.

The enthalpy profile for the nondirected reaction was calculated and is shown in Scheme 11. This profile has a structure similar to those shown in Schemes 4−6. The initial step in the reaction is the complexation of the two reactants,

which is followed by the cycloaddition. In this case the cycloaddition is more synchronous, with the two C−C bonds forming at approximately the same time, leading to a bridged intermediate, which evolves CO$_2$ to yield the final product. Comparison of Scheme 11 with Schemes 4−6 shows that the effective barrier for the nondirected Diels−Alder reaction pathway is much higher than those for the directed Diels−Alder

G

dx.doi.org/10.1021/ja501805r | J. Am. Chem. Soc. XXXX, XXX, XXX−XXX

Scheme 10. Alkynylboronate Diels–Alder Reaction (BPin = Pinacolborane)
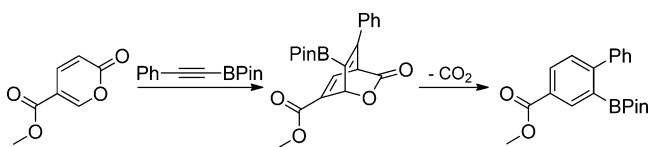
reactions. For the nondirected DA reaction, the TDI is **non-d_DA_I1** for the formation of both products, whereas the TDTS is the cycloaddition transition state in both cases. Thus, the effective enthalpy barrier to generate the more stable product **Pb** is +125.4 kJ mol^{-1}, whereas it is +145.6 kJ mol^{-1} for generating the product **Pa**. From Scheme 11, **Pb** is predicted to be the dominant product because of the significantly lower barrier, which is also confirmed by the experimental observations.

From a consideration of the effective barriers in the three directed Diels–Alder reactions discussed above (varying from +94.0 to +99.7 kJ mol^{-1}), it is clear that the nondirected reaction will require harsher conditions. Moreover, it therefore seems unlikely that this mechanism could operate in parallel with the directed Diels–Alder reaction.

In order to ensure that the above analysis was not specific to the amide substrate **S1**, all of the calculations were repeated with the pyridine-substituted pyrone **1**. The complete reaction profiles for these reactions are given in the Supporting Information. However, the most important data are summarized in Table 3. It is clear from the comparison of the enthalpies for the reactions of the alkynylboron species with **S1** and **1** that

Table 3. Comparison of the Most Relevant Enthalpies (in kJ mol^{-1}) for the Reactions of the Three Alkynylboron Species with Amide S1 and Pyridine-Substituted Pyrone 1

	amide (S1)	pyridine (1)
$\Delta_r H(\text{P-BF2})$	−334.7	−335.0
$\Delta_r H(\text{P-BFR})$	−318.2	−323.8
$\Delta_r H(\text{P-BR2})$	−298.6	−310.5
$\Delta H^{\ddagger}(\text{P-BF2})$	99.7	101.4
$\Delta H^{\ddagger}(\text{P-BFR})$	94.0	91.2
$\Delta H^{\ddagger}(\text{P-BR2})$	95.7	92.2
$\Delta_r H(\text{P-BR2} \rightarrow \text{P-BFR})$	−16.1	−18.5
$\Delta_r H(\text{P-BFR} \rightarrow \text{P-BF2})$	−26.1	−30.3
$\Delta H^{\ddagger}(\text{P-BR2} \rightarrow \text{P-BFR})$	29.5	55.4
$\Delta H^{\ddagger}(\text{P-BFR} \rightarrow \text{P-BF2})$	33.2	62.9

the enthalpic parameters for the reactions with the two substrates are very similar, providing reassurance that the analysis of the reactions with **S1** is applicable to other substrates as well. The calculations also suggest that the reactions with **1** should be faster than the reactions with **S1** under the same conditions. However, the higher barriers for the subsequent disproportionation processes back from **P-BR2** to **P-BF2** should lead to higher conversions to difluoroborane in the case of **S1** versus **1**.[32]

Scheme 11. Enthalpy Profile for the Nondirected Diels–Alder Reaction Shown in Scheme 10
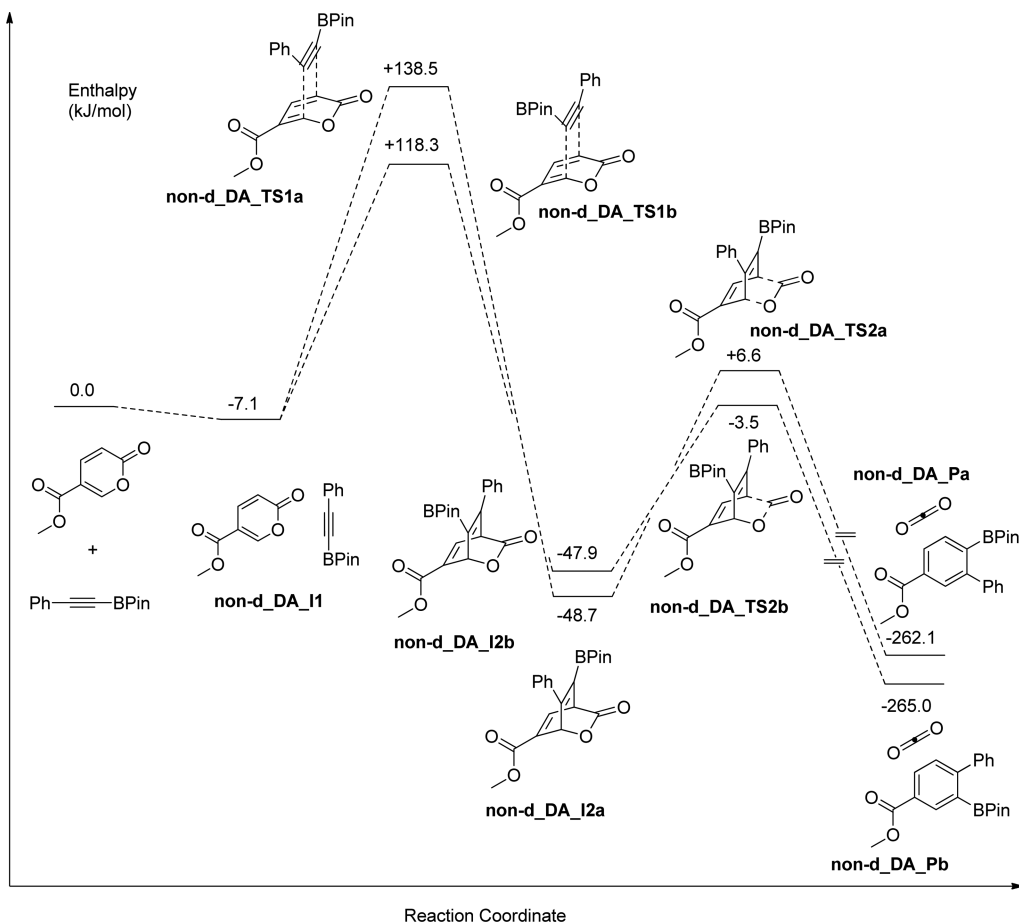
Overall, therefore, our calculations have highlighted three key processes in the boron trifluoride-promoted cycloaddition of alkynyltrifluoroborates and 2-pyrones: (1) rapid pre-equilibration of alkynylboranes through ligand exchange; (2) Lewis acid—base complexation of the dienophile (acid) and diene (base) followed by cycloaddition via a [4 + 2] mechanism; and (3) equilibration of the cycloadducts to a single product, thereby avoiding the formation of product mixtures. It is clear that the precise Lewis acid used should have a significant effect on the effective barriers. Thus, it should be possible to use alternative Lewis acids to modulate these effects, and our investigations toward this end are described at the end of the next section.

■ EXPERIMENTAL RESULTS

Cycloadditions of Alkynylboranes and Pyrones. Our computational investigations highlighted the potential of a mechanism that involved the rapid and reversible formation of a tris(alkynyl)borane followed by cycloaddition and disproportionation. We wanted to confirm the viability of this mechanism experimentally. In this context, Siebert and co-workers reported the synthesis and characterization of tris(*tert*-butylethynyl)borane (**4**) as a Lewis acid—base complex with pyridine,[33] and it occurred to us that we could employ this chemistry to probe the key cycloaddition step. More specifically, if tris(alkynyl)borane **4** was unreactive with pyrone **1**, then we should be able to observe the resulting complex and compare our data with those reported by Siebert. However, if the alkyne was reactive, then we would expect to recover the corresponding cycloadduct **5c** (Scheme 12). In the event that **5c** was isolated, we could confirm the possibility of the final disproportionation process by treating this compound with a boron Lewis acid.

Scheme 12. Complexation or Cycloaddition of Tris(alkynyl)borane 4 and Pyrone 1
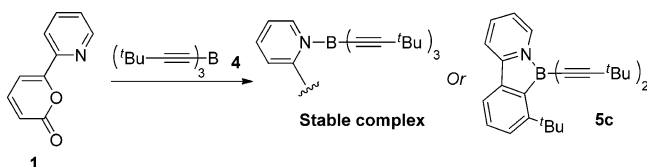
We prepared tris(alkynyl)borane **4** according to the literature procedure and found that it underwent cycloaddition with **1** to generate bis(alkynyl)borane derivative **5c** in 95% yield (Scheme 13). Notably, we did not observe any chloroborane-derived

Scheme 13. Synthesis and Cycloaddition of Tris(alkynyl)borane 4
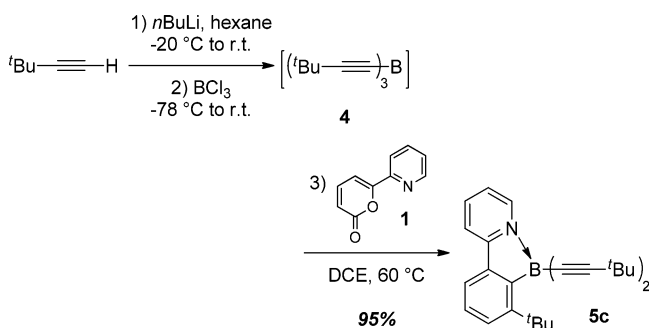
cycloadducts. This result supported our computational results showing that the tris(alkynyl)borane derivative functions as the 2π component in the [4 + 2] cycloaddition between 2-pyrones and potassium (alkynyl)trifluoroborate salts.

Further control experiments were carried out to validate the possibility of the final disproportionation step. We first verified that difluoroborane complex **5a** was obtained upon exposure of bis(alkynyl)borane derivative **5c** to boron trifluoride (Scheme 14). The observation that this process takes place smoothly at

Scheme 14. Equilibration of Bis(alkynyl)borane 5c to Difluoroborane 5a
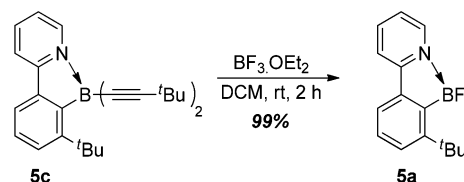
room temperature matches the results of our theoretical study, which predicted the barrier to ligand exchange between BF₃ and the products to be quite small (cf. Scheme 7).

In order to demonstrate the generality of the disproportionation process, complexes **6b** and **6c** were also prepared (Scheme 15). Treatment of pyrone **S1** with trifluoroborate salt **2** in the presence of boron trifluoride for 4 min led to the isolation of **6b** and **6c** in 11% and 17% yield, respectively (Scheme 15a).[34] As expected, difluoroborane **6a** was isolated in 75% yield when a 1:1 mixture of **6b** and **6c** was treated with boron trifluoride (Scheme 15b), further validating the computational results.

Both theoretical and experimental results allow us to propose a mechanism accounting for the transformation (Scheme 16). The rapid establishment of an equilibrium between alkynyldihalogenoborane **A**, bis(alkynyl)halogenoborane **B**, and tris(alkynyl)borane **C** followed by [4 + 2] cycloadditions between the 2-pyrone and the three borane derivatives affords cycloadducts **D**, **E**, and **F**, respectively. Finally, intermediates **E** and **F** are converted into dihalogenoborane cycloadduct **D** by reaction with BX₃.

Extension of the Methodology Using BCl₃. Our theoretical studies indicated that the precise Lewis acid used should have a significant effect on the effective barrier for this reaction. Thus, as implied in the mechanism shown in Scheme 16, it seemed logical that other boron trihalides (BX₃) could act as suitable Lewis acids to promote the cycloaddition process. Indeed, we found that both BCl₃ and BBr₃ can function as effective promoters of the cycloaddition (Scheme 17). Using the reaction conditions initially reported in our previous study [i.e., 3 equiv of potassium alkynyltrifluoroborate **2** and 3 equiv of Lewis acid in refluxing CH₂Cl₂],[9] we isolated cycloadducts **7** and **8** in 89% and 68% yield, respectively.

As BCl₃ appeared to be more promising, an optimization study of the cycloaddition of **1** and **2** was carried out (Table 4). Interestingly, we found that the temperature of the reaction could be reduced to rt or 0 °C without affecting the yield of the isolated product (entries 3 and 4). Furthermore, the number of equivalents of alkyne and BCl₃ could be reduced without significantly reducing the yield of **7** when the reaction was carried at 0 °C (entry 6). This temperature was found to be optimal since a higher or lower reaction temperature (entries 5 and 7) led to a decrease in the isolated yield of **7**. Further

Scheme 15. (a) Synthesis of Alkynylboranes 6b and 6c and (b) Their Equilibration to Difluoroborane 6a
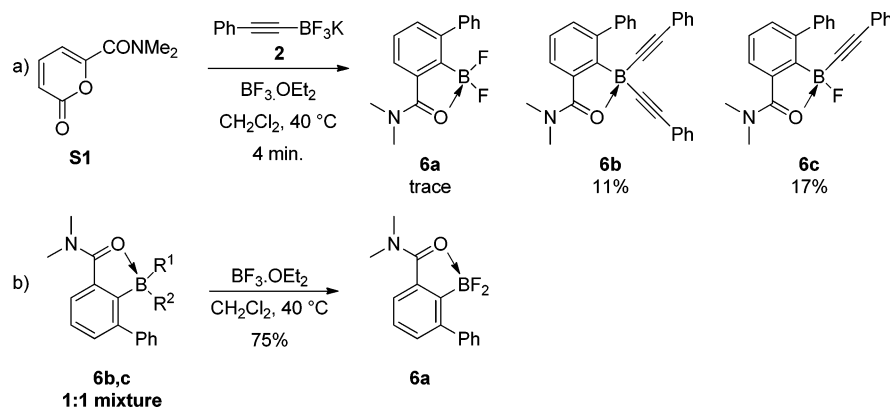
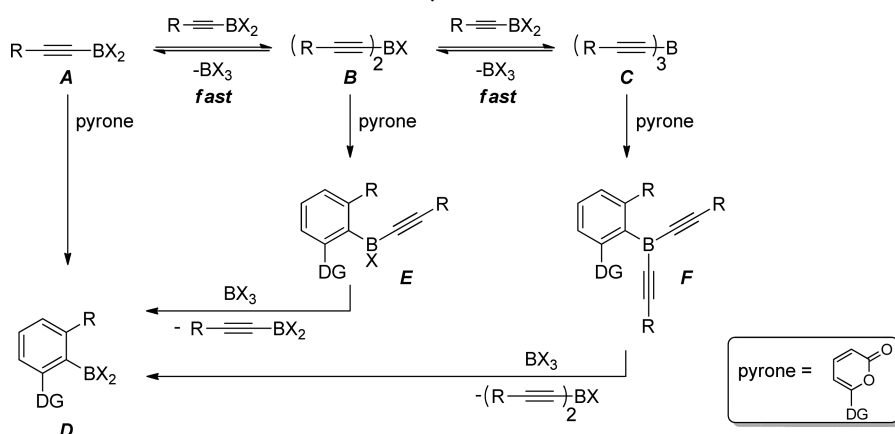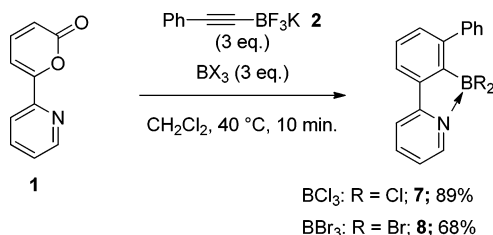**Scheme 16. Overall Mechanistic Scheme for the Directed Cycloaddition Reaction**

Scheme 17. Use of Alterative BX_3 Promoters

BCl₃: R = Cl; **7**; 89%
BBr₃: R = Br; **8**; 68%

Table 4. Lewis Acid Screening

R = F, **3a**
R = Cl, **7**

Entry	BX_3	alkyne / BX_3 n eq. / n eq.	T°C	R	Isolated yield %	
1	BF_3	3 / 3	40	F	82%	initial conditions
2	BCl_3	3 / 3	40	Cl	89%	
3	BCl_3	3 / 3	r.t.	Cl	84%	
4	BCl_3	3 / 3	0	Cl	93%	
5	BCl_3	2 / 2	r.t	Cl	68%	
6	BCl_3	2 / 2	0	Cl	84%	
7	BCl_3	2 / 2	-15	Cl	78%	

reduction of the number of equivalents of alkyne and BCl_3 gave incomplete conversions after prolonged reaction times. Overall, this study demonstrated that higher reactivity could be achieved when BCl_3 was used as the reaction promoter.

The reaction scope was next investigated using our optimized conditions (i.e., 2 equiv of potassium alkynyltrifluoroborate and 2 equiv of BCl_3). First, we prepared a series of potassium alkynyltrifluoroborate salts and used them in the cycloaddition reaction with 2-pyrones **1** and **20** (Table 5). Similar trends were obtained in the two cases. Alkyne substrates bearing phenyl, *n*-butyl, and *tert*-butyl substituents reacted rapidly under mild conditions to give the corresponding functionalized aromatic products **7** and **12−19** in good to excellent yields (entries 1−8). The combination of thiazole-substituted 2-pyrone **20** and trimethylsilyl (TMS)-substituted alkyne **11** resulted in a slower reaction, and this process was conducted at slightly elevated temperature, resulting in some protodesilylation of the product.

The cycloadditions with 2-pyrones attached at the 4-position of various 1,3-azole groups was found to be more challenging, and these reactions were generally conducted at elevated temperature (Table 6). Nonetheless, these reactions allow a range of biaryl products to be accessed in good yields. Pyrone **21**, which is a regioisomer of pyrone **20** from Table 5, also underwent the cycloaddition with alkynes **2**, **8**, and **10** (entries 1−3). Pyrone **22** having 2-methyloxazole as the directing group was also efficient under our reaction conditions, affording products **27−29** in good yields (entries 4−6). Interestingly, a small change in the 2-methyloxazole motif showed a dramatic

Table 5. Cycloaddition Scope

Entry	Pyrone	R^2	T °C	Product	Isolated yield	Entry	Pyrone	R^2	T °C	Product	Isolated yield
1	**1**	Ph- (**2**)	0 °C	**7**	84%	6		Ph- (**2**)	0 °C	**16**	83%
2		^{n}Bu- (**8**)	0 °C	**12**	89%	7		^{n}Bu- (**8**)	0 °C	**17**	97%
3		^{t}Bu- (**9**)	0 °C	**13**	70%	8	**20**	1-cyclo hexenyl- (**10**)	0 °C	**18**	84%
4		1-cyclo hexenyl- (**10**)	0 °C	**14**	54%	9		TMS- (**11**)	40 °C	**19**	51%^{a}
5		TMS- (**11**)	0 °C	**15**	47%						

^{a}The product of protodesilylation was also observed in 18% yield.

Table 6. Cycloaddition Scope

Entry	Pyrone	R^2	time	Product	Isolated yield
1	**21**	Ph- (**2**)	10 min.	**24**	77%
2		^{n}Bu- (**8**)	10 min.	**25**	75%
3		1-cyclo hexenyl- (**10**)	10 min.	**26**	67%
4	**22**	Ph- (**2**)	10 min.	**27**	76%
5		^{n}Bu- (**8**)	10 min.	**28**	78%
6		1-cyclo hexenyl- (**10**)	10 min.	**29**	48%
7	**23**	Ph- (**2**)	3 d.	**30**	55%
8		^{n}Bu- (**8**)	3 d.	**31**	53%^{a}
9		1-cyclo hexenyl- (**10**)	3 d.	**32**	42%^{a}

^{a}These reactions failed to reach full conversion.

change in reactivity, as 2-pyrone **23** proved to be reluctant to undergo the cycloaddition, requiring a reaction time of 3 days and affording cycloadducts **30**−**32** in modest yields (entries 7−9). Notably, however, attempts to mediate the reaction of **23** and **2** with BF$_3$·OEt$_2$ failed to deliver any product, and only the starting 2-pyrone was returned in this case, highlighting the potential of BCl$_3$ to offer enhanced reactivities.

■ CONCLUSION

We have carried out theoretical and experimental studies of the mechanism of a Lewis acid-promoted cycloaddition of alkynyltrifluoroborates and 2-pyrones bearing a Lewis base promoter. Calculations show that rapid equilibration of in situ-generated alkynyldifluoroboranes takes place to provide low concentrations of the corresponding bis- and tris(alkynyl)-boranes. These latter two species undergo very rapid reaction

via coordination of the Lewis basic donor and a [4 + 2] cycloaddition, which is followed by disproportionation to generate the observed aryldifluoroborane products. The reactions can be further enhanced by the use of BCl$_3$, which allows cycloaddition to take place within 10 min at 0 °C to generate a range of functionalized aromatic products in high yields.

■ ASSOCIATED CONTENT

Ⓢ Supporting Information
General experimental protocols, NMR spectra, and computational data, including Cartesian coordinates (in XYZ format) and energies. This material is available free of charge via the Internet at http://pubs.acs.org.

Ⓦ Web-Enhanced Feature
An animation of the transition state **IM_DA_TS1** is available in the HTML version of this article.

■ AUTHOR INFORMATION

Corresponding Authors
a.meijer@sheffield.ac.uk
j.harrity@sheffield.ac.uk

Notes
The authors declare no competing financial interest.

■ ACKNOWLEDGMENTS

■ REFERENCES

(1) Woodard, B. T.; Posner, G. H. *Adv. Cycloaddit.* **1999**, *5*, 47.
(2) Diels, O.; Alder, K. *Ann. Chem.* **1931**, *490*, 257.
(3) Afarinkia, K.; Vinader, V.; Nelson, T. D.; Posner, G. H. *Tetrahedron* **1992**, *48*, 9111.
(4) (a) Delaney, P. M.; Moore, J. E. *Chem. Commun.* **2006**, 3323. (b) Delaney, P. M.; Browne, D. L.; Adams, H.; Plant, A.; Harrity, J. P. A. *Tetrahedron* **2008**, *64*, 866.
(5) Evnin, A.; Seyferth, D. *J. Org. Chem.* **1967**, *32*, 952.

(6) Seyferth, D.; White, D. *J. Organomet. Chem.* **1972**, *34*, 119.

(7) Kranjc, K.; Štefane, B.; Polanc, S.; Kočevar, M. *J. Org. Chem.* **2004**, *69*, 3190.

(8) Vivat, J. F.; Adams, H.; Harrity, J. P. A. *Org. Lett.* **2010**, *12*, 160.

(9) Kirkham, J. D.; Butlin, R. J.; Harrity, J. P. A. *Angew. Chem., Int. Ed.* **2012**, *51*, 6402.

(10) (a) Singleton, D. A.; Martinez, J. P. *J. Am. Chem. Soc.* **1990**, *112*, 7423. (b) Singleton, D. A. *J. Am. Chem. Soc.* **1992**, *114*, 6563. (c) Leung, S.-W.; Singleton, D. A. *J. Org. Chem.* **1992**, *57*, 4796. (d) Leung, S.-W.; Singleton, D. A. *J. Org. Chem.* **1997**, *62*, 1955.

(11) For example, see: (a) Sakata, K.; Fujimoto, H. *J. Org. Chem.* **2013**, *78*, 3095. (b) Pham, H. V.; Paton, R. S.; Ross, A. G.; Danishefsky, S. J.; Houk, K. N. *J. Am. Chem. Soc.* **2014**, *136*, 2397. (c) Birney, D. M.; Houk, K. N. *J. Am. Chem. Soc.* **1990**, *112*, 4127. (d) Domingo, L. R.; Arnó, M.; Sáez, J. A. *J. Org. Chem.* **2009**, *74*, 5934. (e) Domingo, L. R. *Org. Chem.: Curr. Res.* **2013**, *2*, 120. (f) Soto-Delgado, J.; Saez, J. A.; Tapia, R. A.; Domingo, L. R. *Org. Biomol. Chem.* **2013**, *11*, 8357. (g) Arno, M.; Picher, M. T.; Domingo, L. R.; Andres, J. *Chem.—Eur. J.* **2004**, *10*, 4742. (h) Sarotti, A. M. *Org. Biomol. Chem.* **2014**, *12*, 187 and references therein.

(12) (a) Becke, A. D. *Phys. Rev. A* **1988**, *38*, 3098. (b) Becke, A. D. *J. Chem. Phys.* **1993**, *98*, 1372.

(13) Lee, C.; Yang, W.; Parr, R. G. *Phys. Rev. B* **1988**, *37*, 785.

(14) Frisch, M. J.; Trucks, G. W.; Schlegel, H. B.; Scuseria, G. E.; Robb, M. A.; Cheeseman, J. R.; Scalmani, G.; Barone, V.; Mennucci, B.; Petersson, G. A.; Nakatsuji, H.; Caricato, M.; Li, X.; Hratchian, H. P.; Izmaylov, A. F.; Bloino, J.; Zheng, G.; Sonnenberg, J. L.; Hada, M.; Ehara, M.; Toyota, K.; Fukuda, R.; Hasegawa, J.; Ishida, M.; Nakajima, T.; Honda, Y.; Kitao, O.; Nakai, H.; Vreven, T.; Montgomery, J. A., Jr.; Peralta, J. E.; Ogliaro, F.; Bearpark, M.; Heyd, J. J.; Brothers, E.; Kudin, K. N.; Staroverov, V. N.; Kobayashi, R.; Normand, J.; Raghavachari, K.; Rendell, A.; Burant, J. C.; Iyengar, S. S.; Tomasi, J.; Cossi, M.; Rega, N.; Millam, J. M.; Klene, M.; Knox, J. E.; Cross, J. B.; Bakken, V.; Adamo, C.; Jaramillo, J.; Gomperts, R.; Stratmann, R. E.; Yazyev, O.; Austin, A. J.; Cammi, R.; Pomelli, C.; Ochterski, J. W.; Martin, R. L.; Morokuma, K.; Zakrzewski, V. G.; Voth, G. A.; Salvador, P.; Dannenberg, J. J.; Dapprich, S.; Daniels, A. D.; Farkas, Ö.; Foresman, J. B.; Ortiz, J. V.; Cioslowski, J.; Fox, D. J. *Gaussian 09*, revision D.01; Gaussian, Inc.: Wallingford, CT, 2009.

(15) Peng, C.; Schlegel, H. B. *Isr. J. Chem.* **1993**, *33*, 449.

(16) Peng, C.; Ayala, P. Y.; Schlegel, H. B.; Frisch, M. J. *J. Comput. Chem.* **1996**, *17*, 49.

(17) Cances, M. T.; Mennucci, B.; Tomasi, J. *J. Chem. Phys.* **1997**, *107*, 3032.

(18) Schlegel, H. B. *J. Comput. Chem.* **1982**, *3*, 214.

(19) Fukui, K. *Acc. Chem. Res.* **1981**, *14*, 363.

(20) Mennucci, B.; Tomasi, J. *J. Chem. Phys.* **1997**, *106*, 5151.

(21) Cossi, M.; Barone, V.; Mennucci, B.; Tomasi, J. *Chem. Phys. Lett.* **1998**, *286*, 253.

(22) Cossi, M.; Scalmani, G.; Rega, N.; Barone, V. *J. Chem. Phys.* **2002**, *117*, 43.

(23) Sing, U. C.; Kollman, P. A. *J. Comput. Chem.* **1984**, *5*, 129.

(24) Besler, B. H.; Merz, K. M.; Kollman, P. A. *J. Comput. Chem.* **1990**, *11*, 217.

(25) Bardin, V. V.; Adonin, N. Y.; Frohn, H.-J. *J. Fluorine Chem.* **2007**, *128*, 699.

(26) Negishi, E.-i.; Idacavage, M. J.; Chiu, K.-W.; Yoshida, T.; Abramovitch, A.; Goettel, M. E.; Silveira, A.; Bretherick, H. D. *J. Chem. Soc., Perkin Trans. 2* **1978**, 1225.

(27) (a) Cao, Y.; Osuna, S.; Liang, Y.; Haddon, R. C.; Houk, K. N.; Braunschweig, A. B. *J. Am. Chem. Soc.* **2013**, *135*, 9240. (b) Štefane, B.; Perdih, A.; Pevec, A.; Šolmajer, T.; Kočevar, M. *Eur. J. Org. Chem.* **2010**, 5870. (c) Kranjc, K.; Kočevar, M. *New J. Chem.* **2005**, *29*, 1027.

(28) Kozuch, S.; Shaik, S. *Acc. Chem. Res.* **2011**, *44*, 101.

(29) Kozuch, S.; Martin, J. M. L. *ChemPhysChem* **2011**, *12*, 1413.

(30) Kozuch, S. *Wiley Interdiscip. Rev.: Comput. Mol. Sci.* **2012**, *2*, 795.

(31) Kirkham, J. D.; Leach, A. G.; Row, E. C.; Harrity, J. P. A. *Synthesis* **2012**, *44*, 1964.

(32) This is indeed what was found experimentally. When **S1** was mixed with **IM1** for 40 min at room temperature, 70% conversion was obtained with 80% **P-BF2**, 20% **P-BFR**, and only traces of **P-BR2**. When instead **1** was mixed with **IM1** under the same conditions, 92% conversion was achieved with 45% **P-BF2**, 27% **P-BFR**, and 28% **P-BR2** (as estimated by 400 MHz ^{1}H NMR spectroscopy of the crude reaction mixtures).

(33) Bayer, M. J.; Pritzkow, H.; Siebert, W. *Eur. J. Org. Chem.* **2002**, 2069.

(34) The low yields observed in this case can be attributed to the fact that several purifications by column chromatography were required to obtain **8b** and **8c** as clean products.